A model with flavor-dependent gauged $U(1)_{B-L_1}\times U(1)_{B-L_2-L_3}$ symmetry*

Linping Mu(穆林平)[1;1)] Hiroshi Okada[2,3;2)] Chao-Qiang Geng(耿朝强)[1,2,4;3)]

[1]School of Physics and Information Engineering, Shanxi Normal University, Linfen 041004
[2]Physics Division, National Center for Theoretical Sciences, Hsinchu, Taipei 300
[3]Asia Pacific Center for Theoretical Physics, Pohang, Geyoengbuk 790-784
[4]Department of Physics, National Tsing Hua University, Hsinchu, Taipei 300

Abstract: We propose a new model with flavor-dependent gauged $U(1)_{B-L_1}\times U(1)_{B-L_2-L_3}$ symmetry in addition to the flavor-blind symmetry in the Standard Model. The model contains three right-handed neutrinos to cancel gauge anomalies and several Higgs bosons to construct the measured fermion masses. We show the generic features of the model and explore its phenomenology. In particular, we discuss the current bounds on the extra gauge bosons from the K and B meson mixings as well as the LEP and LHC data, and focus on their contributions to the lepton flavor violating processes of $\ell_{i+1}\to\ell_i\gamma$ (i=1,2).

Keywords: flavor-dependent gauged Abelian symmetries, model building, numerical analysis of gauge boson masses and coupling

PACS: 12.60.Cn, 12.60.Fr **DOI:** 10.1088/1674-1137/42/12/123106

1 Introduction

Two vector $U(1)$ gauge bosons often appear in grand unified theories (GUTs) such as $SO(10)$ gauged symmetry [1] when it spontaneously breaks down, when a flavor-blind gauged $U(1)_{B-L}$ can be naturally induced along with right-handed neutrinos. On the other hand, flavor-dependent $U(1)$ gauged symmetries are one of the promising scenarios to explain several anomalies beyond the Standard Model (SM), such as semi-leptonic decays involving $b\to s\ell\bar{\ell}$, the muon anomalous magnetic moment, and so on [2].

In this paper, we propose a new model which contains two extra flavor-dependent gauge symmetries: $U(1)_{B-L_1}\times U(1)_{B-L_2-L_3}$, with the subscript numbers representing family indices besides the flavor-blind SM one. This type of the extension of the SM is, of course, difficult to embed into a larger group such as GUTs. But, due to the flavor dependence, there exist flavor changing processes via vector gauge bosons, resulting in slightly different signatures from typical gauged symmetries such as the flavor-blind $U(1)_{B-L}$ models.

This paper is organized as follows. In Section 2, we first construct our model by showing its field contents and their charge assignments, and then give the concrete renormalizable Lagrangian with scalar and vector gauge boson sectors. After that, we discuss the phenomenology, including the interaction terms, the bounds from the K and B meson mixings, the LEP [3] and LHC [4] experiments, and lepton flavor violations (LFVs). In Section 3, we perform numerical analysis. In Section 4, we extend our model to explain several anomalies indicated by current experiments. Finally, we conclude in Section 5 with some discussion.

2 Model setup and phenomenology

First of all, we impose two additional $U(1)_{B-L_1}\times U(1)_{B-L_2-L_3}$ gauge symmetries by including three right-handed neutral fermions $N_{R_{1,2,3}}$, with the subscripts representing the family indices. The field contents of the fermions and scalar bosons are given in Tables 1 and 2 respectively. Then, the anomaly cancellations among $U(1)^3_{B-L_1}$, $U(1)_{B-L_1}$, $U(1)^3_{B-L_2-L_3}$, $U(1)_{B-L_2-L_3}$,

Received 18 June 2018, Revised 2 September 2018, Published online 30 October 2018

∗ Supported by National Center for Theoretical Sciences and MoST (MoST-104-2112-M-007-003-MY3 and MoST-107-2119-M-007-013-MY3)

1) E-mail: mulinping6266@163.com

2) E-mail: okada.hiroshi@apctp.org

3) E-mail: geng@phys.nthu.edu.tw

Table 1. Field contents of fermions and their charge assignments under $SU(3)_C\times SU(2)_L\times U(1)_Y\times U(1)_{B-L_1}\times U(1)_{B-L_2-L_3}$, where the subscripts 1 and i=2,3 correspond to the family indices.

Fermions	Q_{L_1}	Q_{L_i}	u_{R_1}	u_{R_i}	d_{R_1}	d_{R_i}	L_{L_1}	L_{L_i}	e_{R_1}	e_{R_i}	N_{R_1}	N_{R_i}
$SU(3)_C$	3	3	3	3	3	3	1	1	1	1	1	1
$SU(2)_L$	2	2	1	1	1	1	2	2	1	1	1	1
$U(1)_Y$	$\frac{1}{6}$	$\frac{1}{6}$	$\frac{2}{3}$	$\frac{2}{3}$	$-\frac{1}{3}$	$-\frac{1}{3}$	$-\frac{1}{2}$	$-\frac{1}{2}$	-1	-1	0	0
$U(1)_{B-L_1}$	$\frac{1}{3}$	0	$\frac{1}{3}$	0	$\frac{1}{3}$	0	-1	0	-1	0	-1	0
$U(1)_{B-L_2-L_3}$	0	$\frac{1}{3}$	0	$\frac{1}{3}$	0	$\frac{1}{3}$	0	-1	0	-1	0	-1

$U(1)^2_{B-L_1}U(1)_Y$, $U(1)_{B-L_1}U(1)^2_Y$, $U(1)^2_{B-L_2-L_3}U(1)_Y$, $U(1)_{B-L_2-L_3}U(1)^2_Y$ are the same as the typical single flavor-independent gauged $U(1)_{B-L}$ symmetry, while those from $U(1)_{B-L_1}\times U(1)^2_{B-L_2-L_3}$ and $U(1)^2_{B-L_1}\times U(1)_{B-L_2-L_3}$ are automatically cancelled because the two additional charge assignments are orthogonal to each other. In Table 2, H_1 is expected to be the SM Higgs, while H_2 is another isospin doublet scalar boson, which plays a role in providing the mixings of the 1-2 and 1-3 components in the CKM matrix, as we will see below. Under these symmetries, the renormalizable Lagrangian for the quark and lepton sectors and scalar potential are given by:

$$\begin{aligned}-\mathcal{L}=&y_u\bar{Q}_{L_1}\tilde{H}_1u_{R_1}+y_{u_{ij}}\bar{Q}_{L_i}\tilde{H}_1u_{R_j}+y'_{u_{i1}}\bar{Q}_{L_i}\tilde{H}_2u_{R_1}+y_d\bar{Q}_{L_1}H_1d_{R_1}+y_{d_{ij}}\bar{Q}_{L_i}H_1d_{R_j}+y'_{d_{1j}}\bar{Q}_{L_1}H_2d_{R_j}\\&+y_\nu\bar{L}_{L_1}\tilde{H}_1N_{R_1}+y_{\nu_{ij}}\bar{L}_{L_i}\tilde{H}_1N_{R_j}+y_\ell\bar{L}_{L_1}H_1e_{R_1}+y_{\ell_{ij}}\bar{L}_{L_i}H_1e_{R_j}\\&+\frac{1}{2}y_{N_{ij}}\varphi_1\bar{N}^C_{R_i}N_{R_j}+\frac{1}{2}y'_{N_i}\varphi_2(\bar{N}^C_{R_1}N_{R_i}+\bar{N}^C_{R_i}N_{R_1})+\text{h.c.},\end{aligned}\tag{1}$$

$$\begin{aligned}V=&\frac{\mu^2_{H_1}}{2}|H_1|^2+\mu^2_{H_2}|H_2|^2+\mu^2_{\varphi_1}|\varphi_1|^2+\mu^2_{\varphi_2}|\varphi_2|^2+\lambda_{H_1}|H_1|^4+\lambda_{H_2}|H_2|^4+\lambda_{\varphi_1}|\varphi_1|^4+\lambda_{\varphi_2}|\varphi_2|^4+\lambda_{H_1H_2}|H_1|^2|H_2|^2\\&+\lambda'_{H_1H_2}|H^\dagger_1H_2|^2+\lambda_{H_1\varphi_1}|H_1|^2|\varphi_1|^2+\lambda_{H_1\varphi_2}|H_1|^2|\varphi_2|^2+\lambda_{H_2\varphi_1}|H_2|^2|\varphi_1|^2+\lambda_{H_2\varphi_2}|H_2|^2|\varphi_2|^2,\end{aligned}\tag{2}$$

respectively, where $\tilde{H}\equiv(i\sigma_2)H^*$, with σ_2 being the second Pauli matrix, and i runs over 2 to 3.

Table 2. Field contents of scalar bosons and their charge assignments under $SU(3)_C\times SU(2)_L\times U(1)_Y\times U(1)_{B-L_1}\times U(1)_{B-L_2-L_3}$.

Bosons	H_1	H_2	φ_1	φ_2
$SU(3)_C$	1	1	1	1
$SU(2)_L$	2	2	1	1
$U(1)_Y$	$\frac{1}{2}$	$\frac{1}{2}$	0	0
$U(1)_{B-L_1}$	0	$\frac{1}{3}$	0	1
$U(1)_{B-L_2-L_3}$	0	$-\frac{1}{3}$	2	1

Scalar sector:

The scalar fields are parameterized as

$$H_i=\begin{bmatrix}w^+_i\\ \dfrac{v_i+h_i+iz_i}{\sqrt{2}}\end{bmatrix},\quad \varphi_i=\frac{v'_i+\varphi_{R_i}+iz_{\varphi_i}}{\sqrt{2}},\ (i=1,2),\tag{3}$$

with all four CP-odd bosons $z_{1,2,\varphi_1,\varphi_2}$ massless, in which three of them are absorbed by vector gauged bosons $Z_{\rm SM}$, Z' and Z'', respectively, where $Z_{\rm SM}\equiv(g^2_1+g^2_2)v/4$ with $v\equiv\sqrt{v^2_1+v^2_2}\approx 246$ GeV, and $Z'(Z'')$ arises from $U(1)_{B-L_1}(U(1)_{B-L_2-L_3})$[1]. The features of the singly charged bosons are the same as in the typical two-Higgs doublet model. Consequently, the mass-squared, mixing and eigenvalue-squared matrices are found to be

$$M^2_C=\frac{\lambda'_{H_1H_2}}{2}\begin{bmatrix}v^2_2 & v_1v_2\\ v_1v_2 & v^2_1\end{bmatrix},\tag{4}$$

$$O_C=\begin{bmatrix}c_\beta & s_\beta\\ -s_\beta & c_\beta\end{bmatrix},\tag{5}$$

$$D^2_C=\text{Diag}\left[0,\frac{\lambda'_{H_1H_2}v^2}{2}\right],\tag{6}$$

respectively, where the above massless eigenstate is absorbed by the SM gauge boson $W^\pm$, and $c_\beta(s_\beta)=\cos\beta(\sin\beta)$ with $\tan\beta\equiv v_1/v_2$. As for the CP-even sector in the basis of $[h_1,h_2,\varphi_{R_1},\varphi_{R_2}]^t$, we get a four-by-four mass matrix squared M^2_R, which can be diagonalized by the mixing matrix O_R as $D[H_1,H_2,H_3,H_4]\equiv O_RM^2_RO^T_R$,

1) We remark that the dangerous physical Goldstone boson from H_2 can be evaded by introducing an isospin singlet boson φ_3 of (-1/3,1/3) under $U(1)_{B-L_1}\times U(1)_{B-L_2-L_3}$, resulting in additional terms $(H^\dagger_1H_2)\varphi_3$ and $\varphi^*_1\varphi_2\varphi^3_3/\Lambda$ that give the non-vanishing CP-odd mass. Here, Λ is the cut-off scale, expected to be $\mathcal{O}(100)$ TeV at most. Then, the CP-odd Higgs mass with $\mathcal{O}(100)$ GeV is found. Even though φ_3 affects the vector gauge boson masses, we neglect the contribution hereafter, by assuming $v'_{\varphi_3}<<v'_{\varphi_{1,2}}$. Note here that φ_3 does not contribute to the fermion masses.

leading to $[h_1,h_2,\varphi_{R_1},\varphi_{R_2}]^t=O_R^T[H_1,H_2,H_3,H_4]^t$. Here, we identify $H_1\equiv h_{\rm SM}$.

Fermion sector:

The SM Dirac fermions are diagonalized by bi-unitary mixing matrices as $D_{u,d,e}=(U_{u,d,e})_L m_u (U^\dagger_{u,d,e})_R$, and the active neutrinos are derived by an unitary mixing matrix as $D_\nu = U^*_\nu m_\nu U^\dagger_\nu$, while the observed mixing matrices can be defined by $V_{\rm CKM}\equiv U^\dagger_{uL}U_{dL}$, and $V_{\rm MSN}\equiv U^\dagger_\nu U_{eL}$, respectively [5]. However, we impose $U_{uL}=1$ for simplicity. Hence, we reduce the formula to $V_{\rm CKM}\equiv U_{dL}$. In the lepton sector, we classify the case of $V_{\rm MSN}\approx U^\dagger_\nu$ or $V_{\rm MSN}\approx U_{eL}$ below. Here, the neutrino mass matrix m_ν is induced via the canonical seesaw mechanism in Eq. (1).

2.1 Neutral gauge boson sector

$Z_{\rm SM}$-Z'-Z'' mixing: Since H_2 and $\varphi_{1,2}$ have nonzero $U(1)_{B-L_1}$ and $U(1)_{B-L_2-L_3}$ charges, there are mixings among $Z_{\rm SM}$, Z' and Z''. The resulting mass matrix in the basis of $(Z_{\rm SM},Z',Z'')$ is given by

$$m^2_{Z_{\rm SM},Z',Z''} = \begin{bmatrix} \frac{g^2v^2}{4} & -\frac{1}{6}g'_1gv_2^2 & \frac{1}{6}g'_2gv_2^2 \\ -\frac{1}{6}g'_1gv_2^2 & \frac{1}{9}g'^2_1(v_2^2+9v'^2_2) & -\frac{1}{9}g'_1g'_2(v_2^2-9v'^2_2) \\ \frac{1}{6}g'_2gv_2^2 & -\frac{1}{9}g'_1g'_2(v_2^2-9v'^2_2) & \frac{1}{9}g'^2_2[v_2^2+9(4v'^2_1+v'^2_2)] \end{bmatrix}, \tag{7}$$

where $g^2\equiv g_1^2+g_2^2$, $m_{Z_{\rm SM}}\equiv\frac{\sqrt{g_1^2+g_2^2}v}{2}\approx 91.18$ GeV, and g_1, g_2, g'_1 and g'_2 are the gauge couplings of $U(1)_Y$, $SU(2)_L$, $U(1)_{B-L_1}$ and $U(1)_{B-L_2-L_3}$, respectively. Here, we can identify the mass of Z_1 as the SM one, since we expect $v_2<<v_1<v'_{1,2}$ in order to reproduce the SM fermion masses and the LEP measurement of $m_{Z_1}\sim m_{Z_{\rm SM}}$. This approximation is in good agreement with the current experimental data, as the mass difference between $m_{Z_{\rm SM}}$ and m_{Z_1} should be less than $O(10^{-3})$ GeV.

The other part can be reduced to

$$m^2_{Z',Z''}\sim\begin{bmatrix} g'^2_1v'^2_2 & g'_1g'_2v'^2_2 \\ g'_1g'_2v'^2_2 & g'^2_2(4v'^2_1+v'^2_2) \end{bmatrix}, \tag{8}$$

which is diagonalized by the two-by-two mixing matrix V_G as $V_G m^2_{Z',Z''}V_G^T\equiv{\rm Diag}(m^2_{Z'_1},m^2_{Z'_2})$, with

$$m^2_{Z'_1}=\frac{1}{2}\Big[g'^2_2(4v'^2_1+v'^2_2)+g'^2_1v'^2_2 - \sqrt{g'^4_2(4v'^2_1+v'^2_2)^2+g'^4_1v'^4_2+2g'^2_1g'^2_2v'^2_2(-4v'^2_1+v'^2_2)}\Big], \tag{9}$$

$$m^2_{Z'_2}=\frac{1}{2}\Big[g'^2_2(4v'^2_1+v'^2_2)+g'^2_1v'^2_2 + \sqrt{g'^4_2(4v'^2_1+v'^2_2)^2+g'^4_1v'^4_2+2g'^2_1g'^2_2v'^2_2(-4v'^2_1+v'^2_2)}\Big], \tag{10}$$

$$V_G=\begin{bmatrix} c_\theta & s_\theta \\ -s_\theta & c_\theta \end{bmatrix},\quad s_\theta=\frac{1}{\sqrt{2}}\sqrt{1+\frac{g'^2_2(4v'^2_1+v'^2_2)-g'^2_1v'^2_2}{m^2_{Z'_2}-m^2_{Z'_1}}}. \tag{11}$$

Note here that we have to satisfy the following condition:

$$16g'^2_1g'^2_2v'^2_1v'^2_2\le[g'^2_1v'^2_2+g'^2_2(4v'^2_1+v'^2_2)]^2, \tag{12}$$

that arises from the need for the vector boson masses to be positive real.

Here, we evaluate the typical scale of v_2 that should be suppressed by the deviation of m_{Z_1} from $m_{Z_{\rm SM}}$ at the next leading order, $\delta m_Z\equiv|m_{Z_1}-m_{Z_{\rm SM}}|$, approximately given by

$$\delta m_Z^2\sim\frac{g^2v_2^4}{72}\left(\frac{|g'_1\sqrt{1-X}+g'_2\sqrt{1+X}|^2}{m^2_{Z_{\rm SM}}-m^2_{Z'_1}} + \frac{|g'_1\sqrt{1+X}-g'_2\sqrt{1-X}|^2}{m^2_{Z_{\rm SM}}-m^2_{Z'_2}}\right), \tag{13}$$

$$X=\frac{g'^2_2(4v'^2_1+v'^2_2)-g'^2_1v'^2_2}{m^2_{Z'_2}-m^2_{Z'_1}}, \tag{14}$$

where δm_Z should satisfy $\delta m_Z\lesssim 2.1\times10^{-3}$ GeV from the electroweak precision test. As a result, we find, e.g., $v_2\lesssim 19.5$ GeV for $v'_{1,2}\sim10^5$ GeV and $g'_{1,2}\sim10^{-3}$.

Interacting Lagrangian: The interactions in the kinetic term between the neutral vector bosons and quarks in terms of the mass eigenstates are given by:

$$\mathcal{L}_q=-\frac{1}{3}\left[(g'_1c_\theta+g'_2s_\theta)\bar u\gamma^\mu uZ'_{1\mu}+(-g'_1s_\theta+g'_2c_\theta)\sum_{i=c,t}\bar u_i\gamma^\mu u_iZ'_{2\mu}\right] -\frac{1}{3}\left[\bar d_i\gamma^\mu(g'_1c_\theta O_{dZ'}+g'_2s_\theta O_{dZ''})_{ij}d_jZ'_{1\mu}+\bar d_i\gamma^\mu(-g'_1s_\theta O_{dZ'}+g'_2c_\theta O_{dZ''})_{ij}d_jZ'_{2\mu}\right], \tag{15}$$

$$O_{dZ'}=V_{\rm CKM}{\rm diag}(1,0,0)V^\dagger_{\rm CKM}\approx\begin{bmatrix} 0.95 & -0.22 & 0.013+0.0032i \\ -0.22 & 0.0509 & -0.0030-0.00075i \\ 0.013-0.0032i & -0.0030+0.00075i & 0.00019 \end{bmatrix}, \tag{16}$$

$$O_{dZ''}=V_{\rm CKM}{\rm diag}(0,1,1)V^{\dagger}_{\rm CKM}\approx\begin{bmatrix}0.051 & 0.22-0.00014i & -0.0082-0.0033i\\ 0.22+0.00014i & 0.95 & -0.0030-0.00075i\\ -0.0082+0.0033i & -0.0030+0.00075i & 1.0\end{bmatrix}, \tag{17}$$

where we have used the central values for the CKM elements in $V_{\rm CKM}$ [6]. The interactions between the neutral vector bosons and charged-leptons depend on the parameterizations of $V_{\rm MNS}$, given by:

$$V_{\rm MNS}\approx U^{\dagger}_{\nu}:\quad \mathcal{L}^{(1)}_{\ell}=\left[(g'_1c_\theta+g'_2s_\theta)\bar{e}\gamma^\mu eZ'_{1\mu}+(-g'_1s_\theta+g'_2c_\theta)\sum_{i=\mu,\tau}\bar{\ell}_i\gamma^\mu\ell_iZ'_{2\mu}\right], \tag{18}$$

$$V_{\rm MNS}\approx U_{eL}:\quad \mathcal{L}^{(2)}_{\ell}=\left[\bar{\ell}_i\gamma^\mu(g'_1c_\theta O_{\ell Z'}+g'_2s_\theta O_{\ell Z''})_{ij}\ell_jZ'_{1\mu}+\bar{\ell}_i\gamma^\mu(-g'_1s_\theta O_{\ell Z'}+g'_2c_\theta O_{\ell Z''})_{ij}\ell_jZ'_{2\mu}\right], \tag{19}$$

with $\ell_{i,j}=(e,\mu,\tau)$, where $O_{\ell Z',\ell Z''}$ are derived as

$$O_{\ell Z'}=V_{\rm MNS}{\rm diag}(1,0,0)V^{\dagger}_{\rm MNS}\approx\begin{bmatrix}0.69 & -0.31-0.060i & 0.33-0.068i\\ -0.31+0.060i & 0.14 & -0.14+0.060i\\ 0.33+0.068i & -0.14-0.060i & 0.17\end{bmatrix}, \tag{20}$$

and

$$O_{\ell Z''}=V_{\rm MNS}{\rm diag}(0,1,1)V^{\dagger}_{\rm MNS}\approx\begin{bmatrix}0.31 & 0.31+0.060i & 0.33+0.068i\\ 0.31-0.060i & 0.86 & 0.14-0.060i\\ 0.33-0.068i & 0.14+0.060i & 0.83\end{bmatrix}, \tag{21}$$

respectively, by taking the best fitted results in Ref. [6] for $V_{\rm MNS}$.

2.2 Phenomenology

Since $Z'_{1,2}$ interact with the SM fermions in a non-universal manner, as discussed before, the constraints are unlikely to be the same as those in the typical $U(1)_{B-L}$ models. Here, we will examine the bounds on the extra gauge bosons from the K and B meson mixings as well as the LEP data, and discuss the lepton flavor violating processes of $\ell_{i+1}\to\ell_i\gamma$ (i=1 and 2).

1. $M-\overline{M}$ meson mixings

The extra gauge bosons induce the neutral meson (M)-antimeson ($\overline{M}$) mixings with $M=(K^0,B_d,B_s)$, such as $K^0-\bar{K}^0$, $B_d-\bar{B}_d$, and $B_s-\bar{B}_s$, at the tree level. The formulas for the mass splittings are given by [7]

$$\Delta m_M\approx\left[\frac{|(g'_1c_\theta O_{dZ'}+g'_2s_\theta O_{dZ''})_{21}|^2}{m^2_{Z'_1}}+\frac{|(-g'_1s_\theta O_{dZ'}g'_2c_\theta O_{dZ''})_{21}|^2}{m^2_{Z'_2}}\right]\times m_Mf^2_M\left[\frac{5}{12}-\frac{1}{4}\left(\frac{m_M}{m_q+m_{q'}}\right)^2\right], \tag{22}$$

for $M=(K^0,B_d,B_s)$ with $qq'=(ds,db,ds)$, which should be less than the experimental values of $(3.48\times10^{-4},3.33\times10^{-2},1.17)\times10^{-11}$ GeV [6], where $f_M=(156,191,200)$ MeV and $m_M=(0.498,5.280,5.367)$ GeV.

2. Bounds on $Z'_{1,2}$ from LEP and LHC

From Eqs. (18) and (19), we obtain the effective Lagrangians as:

$$V_{\rm MNS}\approx U^{\dagger}_{\nu}:\ \mathcal{L}^{(1)}_{\rm eff}=\frac{1}{2}\frac{G^2_1}{m^2_{Z'_1}}(\bar{e}\gamma^\mu e)(\bar{e}\gamma_\mu e)+\frac{G_1(V^d_1)_{dd}}{3m^2_{Z'_1}}(\bar{e}\gamma^\mu e)(\bar{d}\gamma_\mu d)+\frac{G^2_1}{3m^2_{Z'_1}}(\bar{e}\gamma^\mu e)(\bar{u}\gamma_\mu u),$$

$$V_{\rm MNS}\approx U_{eL}:\ \mathcal{L}^{(2)}_{\rm eff}=\sum_{i=1,2}\left[\frac{1}{2}\frac{(V^\ell_{ee})^2_i}{m^2_{Z'_i}}(\bar{e}\gamma^\mu e)(\bar{e}\gamma_\mu e)+\sum_{\ell'=\mu,\tau}\frac{(V^\ell_{ee})_i(V^\ell_{\ell'\ell'})_i}{m^2_{Z'_i}}(\bar{e}\gamma^\mu e)(\bar{\ell}'\gamma_\mu\ell')\right. \tag{23}$$

$$\left.+\sum_{q'=d,s,b}\frac{(V^\ell_{ee})_i(V^d_{q'q'})_i}{3m^2_{Z'_i}}(\bar{e}\gamma^\mu e)(\bar{q}'\gamma_\mu q')+\frac{(V^\ell_{ee})_iG_i}{3m^2_{Z'_i}}(\bar{e}\gamma^\mu e)(\bar{u}\gamma_\mu u)\right], \tag{24}$$

respectively, where $(V_{ij}^{d(\ell)})_1 \equiv (g'_1 c_\theta O_{d(\ell)Z'} + g'_2 s_\theta O_{d(\ell)Z''})$, $(V_{ij}^{d(\ell)})_2 \equiv (-g'_1 s_\theta O_{d(\ell)Z'} + g'_2 c_\theta O_{d(\ell)Z''})$, $G_1 \equiv g'_1 c_\theta + g'_2 s_\theta$, and $G_2 \equiv -g'_1 s_\theta + g'_2 c_\theta$. As a results, the bounds for $Z'_{1,2}$ from the measurements of $e^+e^- \to f\bar{f}$ at LEP [3] and $q\bar{q} \to e\bar{e}(\mu\bar{\mu})$ at LHC [4] are found to be

$$V_{\rm MNS} \approx U_\nu^\dagger: \ \frac{(20.6{\rm TeV})^2}{8\pi} \lesssim \frac{m_{Z'_1}^2}{G_1^2},$$
$$\frac{(11.4{\rm TeV})^2}{12\pi} \lesssim \frac{m_{Z'_1}^2}{G_1 (V_1^d)_{dd}} \quad \text{for LEP;} \tag{25}$$
$$\frac{(37{\rm TeV})^2}{12\pi} \lesssim \frac{m_{Z'_1}^2}{G_1^2 + (V_1^d)_{dd} G_1},$$
$$\frac{(30{\rm TeV})^2}{12\pi} \lesssim \frac{m_{Z'_1}^2}{G_2^2 + (V_2^d)_{dd} G_2} \ \text{for LHC,} \tag{26}$$

and

$$V_{\rm MNS} \approx U_{eL}: \ \frac{(20.6{\rm TeV})^2}{8\pi} \lesssim \sum_{i=1,2} \frac{m_{Z'_i}^2}{(V_{ee}^\ell)_i^2},$$
$$\frac{(18.9{\rm TeV})^2}{4\pi} \lesssim \sum_{i=1,2} \frac{m_{Z'_i}^2}{(V_{ee}^\ell)_i (V_{\mu\mu}^\ell)_i},$$
$$\frac{(15.8{\rm TeV})^2}{4\pi} \lesssim \sum_{i=1,2} \frac{m_{Z'_i}^2}{(V_{ee}^\ell)_i (V_{\tau\tau}^\ell)_i},$$
$$\frac{(11.4{\rm TeV})^2}{12\pi} \lesssim \sum_{i=1,2} \frac{m_{Z'_i}^2}{(V_{ee}^\ell)_i (V_{dd}^d)_i},$$
$$\frac{(16.2{\rm TeV})^2}{12\pi} \lesssim \sum_{i=1,2} \frac{m_{Z'_i}^2}{(V_{ee}^\ell)_i G_i} \ \text{for LEP;} \tag{27}$$
$$\frac{(37{\rm TeV})^2}{12\pi} \lesssim \sum_{i=1,2} \frac{m_{Z'_i}^2}{(V_{ee}^\ell)_i [(V_{dd}^d)_i + G_i]},$$
$$\frac{(30{\rm TeV})^2}{12\pi} \lesssim \sum_{i=1,2} \frac{m_{Z'_i}^2}{(V_{\mu\mu}^\ell)_i [(V_{dd}^d)_i + G_i]} \ \text{for LHC,} \tag{28}$$

where $f = e, \mu, \tau, d$ and u. It is worth mentioning that these neutral gauge boson searches will be carried out by experiments such as the International Linear Collider (ILC) [8], and more stringent constraints should be obtained in the near future.

3. Lepton flavor violating processes

For $V_{\rm MNS} \approx U_\nu^\dagger$, one does not need to consider the lepton flavor violations from the $Z'_{1,2}$ mediations, because the charged leptons are diagonal from the beginning. On the other hand, if $V_{\rm MNS} \approx U_{eL}$, the lepton flavor violating processes due to $Z'_{1,2}$ can be induced. In this case, we get

$${\rm BR}(\ell_b \to \ell_a \gamma) \approx \frac{48\pi^3 \alpha_{em} C_{ba}}{(4\pi)^4 G_F^2}$$
$$\times \left| \frac{1}{8\pi^2} \sum_{k=e,\mu,\tau} \sum_{i=1,2} (V_{\ell_a \ell_k}^\ell)_i (V_{\ell_k \ell_b}^{\ell\dagger})_i F_{II} \left[\frac{m_{\ell_k}^2}{m_{Z'_i}^2} \right] \right|^2, \tag{29}$$
$$F_{II}(r) = \int_0^1 \frac{2rx(1-x)^2}{r(1-x)+x}, \tag{30}$$

where G_F and α_{em} are the Fermi and fine structure constants, respectively, while $C_{\mu e} \approx 1$, $C_{\tau e} \approx 0.1784$ and $C_{\tau\mu} \approx 0.1736$. The current experimental limits are given by [9, 10]:

$${\rm BR}(\mu \to e\gamma) \lesssim 4.2 \times 10^{-13},$$
$${\rm BR}(\tau \to e\gamma) \lesssim 4.4 \times 10^{-8},$$
$${\rm BR}(\tau \to \mu\gamma) \lesssim 3.3 \times 10^{-8}. \tag{31}$$

These constraints are imposed in the numerical analysis below[1)].

3 Numerical analysis

In our numerical analysis, we explore the allowed gauge parameters of $g'_{1,2}$ and $m_{Z'_{1,2}}$ by taking $s_\theta = 0$ and $s_\theta = 1/\sqrt{2}$. We scan the parameter regions as follows:

$$v'_{1,2} \in [10^3, 10^6] \ {\rm GeV}, \quad g'_{1,2} \in [10^{-5}, 1]. \tag{32}$$

$V_{\rm MNS} \approx U_\nu^\dagger$:

In Fig. 1, we show the allowed parameter points in the planes of g'_1-g'_2 and $m_{Z'_1}$-$m_{Z'_2}$, with the left-hand and right-hand plots showing $s_\theta = 0$ and $1/\sqrt{2}$, respectively. The top left plot suggests a wide allowed range of values for $g'_{1,2}$ for $s_\theta = 0$, whereas g'_1 and g'_2 should be degenerate for $s_\theta = 1/\sqrt{2}$. The bottom left plot indicates that any values with $m_{Z'_1} \leq m_{Z'_2}$ are permitted for $s_\theta = 0$, whereas the allowed parameter spaces for both $m_{Z'_1}$ and $m_{Z'_2}$ should be narrow within 10 GeV $\leq m_{Z'_{1,2}} \leq 10^6$ GeV for $s_\theta = 1/\sqrt{2}$.

$V_{\rm MNS} \approx U_{eL}$:

In Fig. 2, similar to Fig. 1, we illustrate the corresponding results for the case of $V_{\rm MNS} \approx U_{eL}$ by including the plots for ${\rm BR}(\tau \to \mu\gamma)$-${\rm BR}(\mu \to e\gamma)$ at the bottom. The generic features for the first two plots from the top left in Fig. 2 are similar to those in Fig. 1. While g'_2 is restricted to be $g'_2 \leq 0.2$, the allowed regions for g'_1-g'_2 and $m_{Z'_1}$-$m_{Z'_2}$ are more degenerate than the case of $V_{\rm MNS} \approx U_\nu^\dagger$ for $s_\theta = 1/\sqrt{2}$. For the lepton flavor violating processes at the bottom in Fig. 2, we see that ${\rm BR}(\mu \to e\gamma)$ reaches the current experimental bound in Eq. (31), which is clearly testable in the near future for both cases of s_θ. However, ${\rm BR}(\tau \to \mu\gamma)$ is much lower than the limit in

1) One can consider the anomalous magnetic moment because of the evading of the stringent constraint of the trident production via the Z' boson (flavor eigenstate) [12]. In our case, its value is of the order 10^{-14}, which is much smaller than the experimental value.

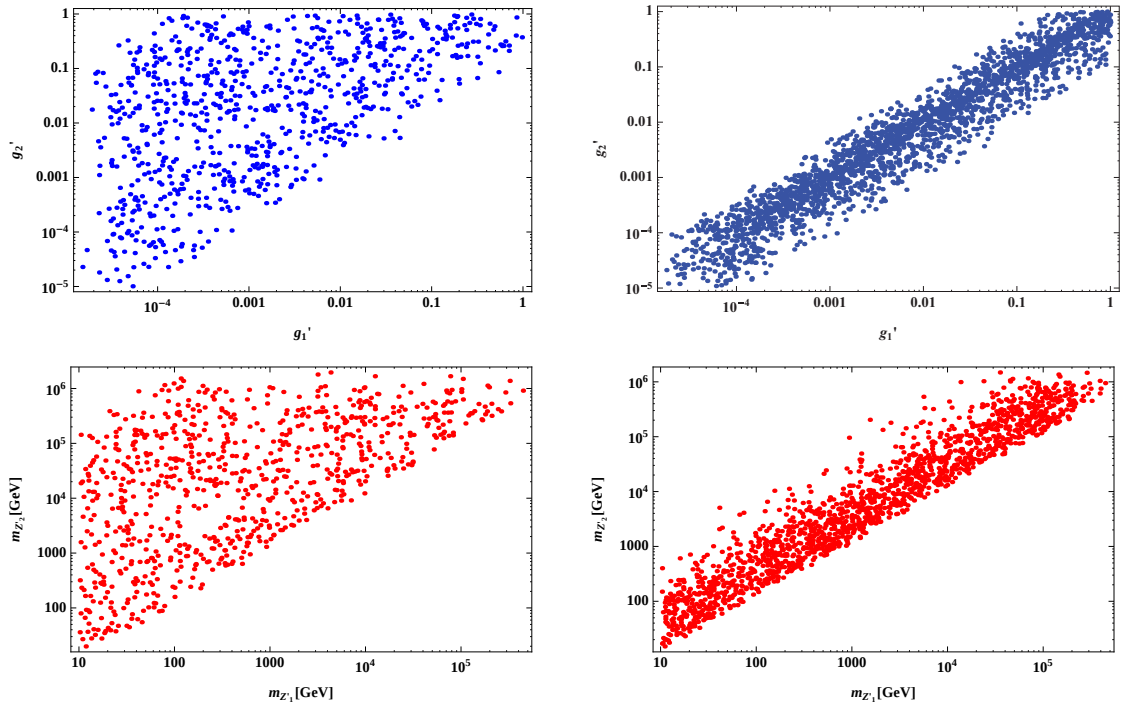

Fig. 1. (color online) Allowed regions in the planes of g_1'-g_2' and $m_{Z_1'}$-$m_{Z_2'}$, where the left-hand and right-hand plots represent s_θ=0 and $1/\sqrt{2}$, respectively, with $V_{\rm MNS}\approx U_\nu^\dagger$.

Eq. (31). Note here that $\mathrm{BR}(\tau\to e\gamma)\approx\mathrm{BR}(\tau\to\mu\gamma)$. We remark that the current bounds on the masses of the extra gauge bosons are around 3 TeV, from the LHC experiments [11][2], consistent with all the cases in our analyses with $g_1'=g_2'=g_Z\approx 0.72$.

Finally, we also mention that the muon anomalous magnetic moment cannot be explained in our present model due to the constraint of the trident production via Z' [12]. Moreover, the new contributions to the semileptonic decays of $b\to s\ell^+\ell^-$ from the $Z'_{1,2}$ mediations are negligibly small, so that our model sheds no light on the recent anomalies in $B\to K^{(*)}\mu^+\mu^-$, unlike the models with an extra Z' in the literature [2]. Thus, we minimally extend our model to explain these issues in the next section.

4 An extension

We now extend our model by introducing two extra vector-like fermions: $Q'_{L/R}=(3,2,1/6,1/2,-2/3)$ and $L'_{L/R}=(1,2,-1/2,1/2,-2)$, along with a neutral inert complex scalar $S=(1,1,0,-1/2,1)$ under $SU(3)_C\times SU(2)_L\times U(1)_Y\times U(1)_{B-L_1}\times U(1)_{B-L_2-L_3}$ [13], resulting in the following additional Lagrangian:

$$\mathcal{L}=f_i\bar{L}_{L_i}L'_R S+g_i\bar{Q}_{L_i}Q'_R S+M_{Q'}\bar{Q}'Q'+M_{L'}\bar{L}'L'+\mathrm{h.c.}, \tag{33}$$

where $i=2,3$. Here, we have assumed the mass eigenstates for the above down-quark and charged-lepton sectors in the SM, and $f_3<<f_2$. As a result, the $b\to se\bar{e}$ excess is negligible, which is consistent with the current experimental data, while $\tau\to\mu\gamma$ at one-loop level is also suppressed to avoid the current experimental bound. Note that S is a complex boson that is assured by the charge assignment under $U(1)_{B-L_1}\times U(1)_{B-L_2-L_3}$, and its mass is denoted by m_S.

Muon anomalous magnetic moment :

The muon anomalous magnetic moment is formulated by :

$$\Delta a_\mu=\frac{|f_2|^2}{8\pi^2}\int_0^1 \mathrm{d}x\frac{x^2(1-x)}{x(x-1)+r_{L'}x+(1-x)r_S}\ , \tag{34}$$

where $r_{L'}\equiv(M_{L'}/m_\mu)^2$ and $r_S\equiv(m_S/m_\mu)^2$. The experimental deviation from the SM at 3.3σ C.L. is given by [14]

$$\Delta a_\mu=(26.1\pm 8.0(16.0))\times 10^{-10}\ . \tag{35}$$

$B\to K^*\bar{\mu}\mu$ anomaly: The effective Hamiltonian for the $b\to s\mu^+\mu^-$ transition is induced via the box diagram [15], given by

$$\mathcal{H}_{\rm eff}(b\to s\mu^+\mu^-)=\frac{(g_2g_3^*)|f_2|^2}{(4\pi)^2}F_{\rm box}(m_S,M_{Q'},M_{L'})\times(\bar{s}\gamma^\rho P_L b)(\bar{\mu}\gamma_\rho\mu-\bar{\mu}\gamma_\rho\gamma_5\mu)+\mathrm{h.c.}$$

2) The LHC bounds are typically stronger than the LEP ones in case of a simple gauged $U(1)_{B-L}$ model.

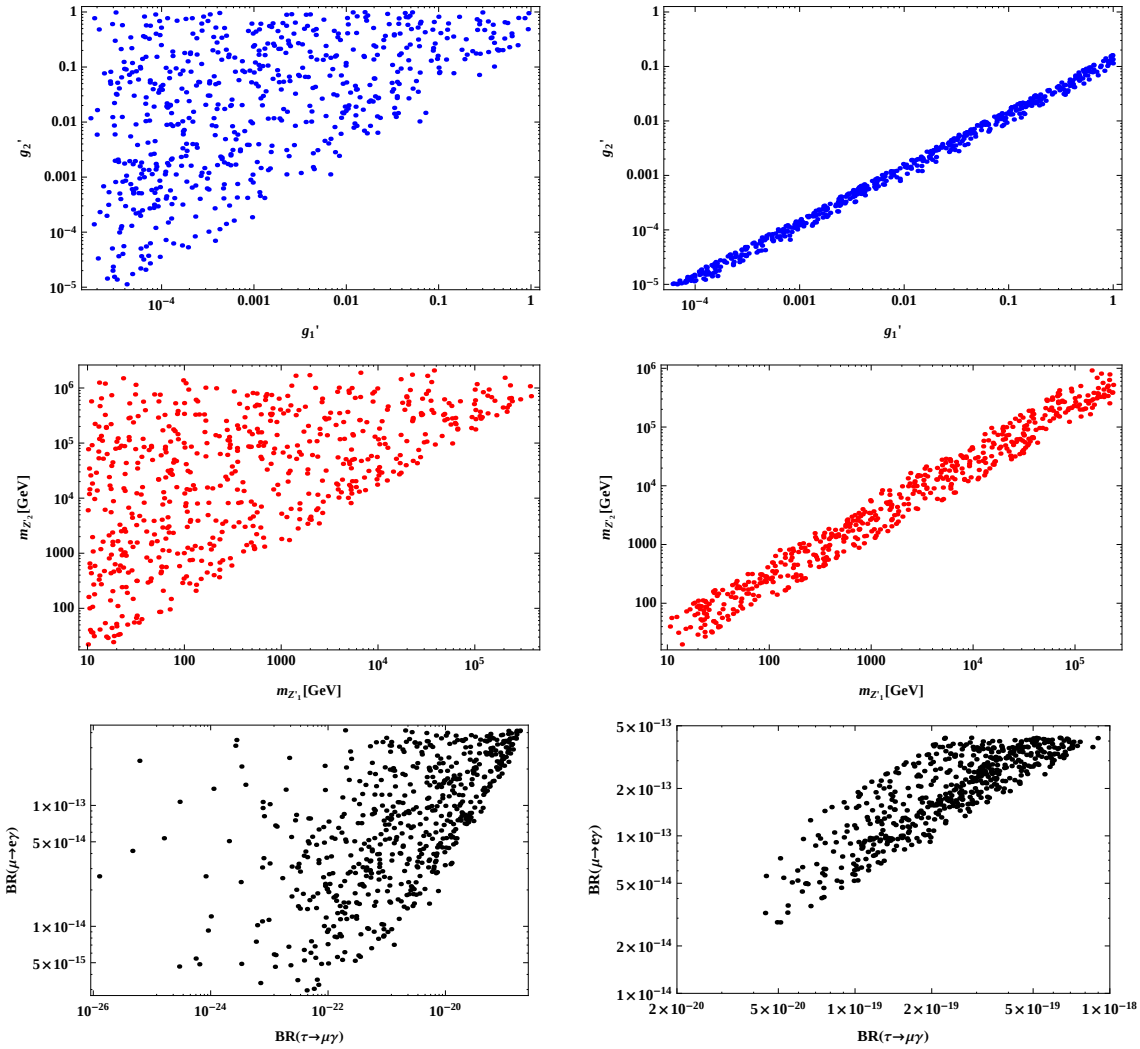

Fig. 2. (color online) Allowed regions in the planes of g_1'-g_2', $m_{Z_1'}$-$m_{Z_2'}$, and BR($\tau\to\mu\gamma$)-BR($\mu\to e\gamma$), where the left-hand and right-hand plots represent $s_\theta=0$ and $1/\sqrt{2}$, respectively, with $V_{\rm MNS}\approx U_{eL}$.

$$\equiv -C_{\rm SM}[C_9O_9-C_{10}O_{10}]+\text{h.c.}, \quad (36)$$

where

$$F_{\rm box}(m_S,M_{Q'},M_{L'}) \approx\frac{1}{2}\int_0^1 {\rm d}x_1\int_0^{1-x_1}{\rm d}x_2\frac{x_1}{x_1m_S^2+x_2M_{Q'}^2+(1-x_1-x_2)M_{L'}^2}, \quad (37)$$

$$C_{\rm SM}\equiv\frac{V_{tb}V_{ts}^*G_F\alpha_{em}}{\sqrt{2}\pi},$$

with $V_{tb}\sim 0.9991$ and $V_{ts}\sim -0.0403$ being the CKM matrix elements [6]. Here, we take $C_9=-C_{10}$, which is one of the promising relations to explain the anomaly [16], and the experimental result is given by

$$[-0.85,-0.50]\text{ at }1\sigma,\quad [-1.22,-0.18]\text{ at }2\sigma, \quad (38)$$

where the best fit value is -0.68.

Neutral meson mixing: The neutral meson mixing gives the bounds on g_i and $M_{Q'}$ at low energy, where our valid process is the $B_s-\bar{B}_s$ mixing in our case. Similar to the $B\to K^*\mu\bar{\mu}$ anomaly, the formula is derived by [7]:

$$\Delta m_{B_s}:\ (g_3g_2^*)(g_2g_3^*)F_{\rm box}(m_S,M_{Q'},M_{Q'})\lesssim 1.17\times10^{-11} \times\frac{24\pi^2}{m_{B_s}f_{B_s}^2}\ \text{GeV}, \quad (39)$$

where the above parameters are found to be $f_{B_s}=0.200$ GeV [7], and $m_{B_s}=5.367$ GeV [6].

Dark matter candidate: We suppose that S is a DM candidate. First, we assume that any annihilation modes coming from the Higgs potential are negligibly small. This is a reasonable assumption, because we can avoid the strong constraint coming from the spin independent scattering cross section reported by several direct DM detection experiments, such as LUX [17]. Second, we do not consider the modes through $Z_{1,2}'$ coming from

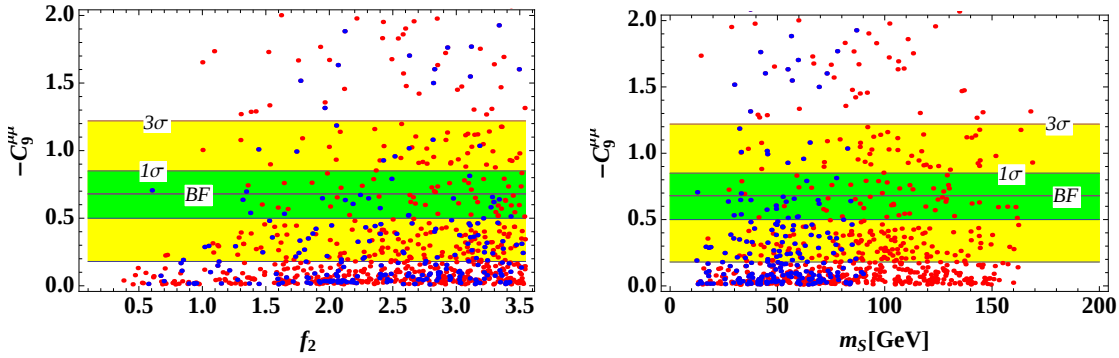

Fig. 3. (color online) Allowed regions, where the left(right)-hand figure represents the $f_2(m_S)--C_9$ plane, and the blue(red) points satisfy muon $g-2$ in the range of $(26.1\pm8.0(16.0))\times10^{-10}$. The yellow(green) region denotes the experimental allowed region [-1.22(-0.85),-0.18(-0.50)] at $1(2)\sigma$, where the black horizontal line inside the green region shows the best fit (BF).

the kinetic term, since this is suppressed enough by the masses of $m_{Z'_{1,2}}$. We comment here that there are two resonant solutions around the points of $m_{Z'_1}=2m_S$ and $m_{Z'_2}=2m_S$. Subsequently, the dominant contribution to the thermal relic density comes from f and g, and the cross section is approximately given by [18]

$$(\sigma v_{\rm rel})\approx\frac{m_S^2}{16\pi}\left(\frac{|f_2|^4}{6(m_S^2+M_{L'}^2)^2}+\sum_{i=2,3}\frac{|g_ig_j|^2}{(m_S^2+M_{Q'}^2)^2}\right)v_{\rm rel}^2 +\mathcal{O}(v_{\rm rel}^4), \quad (40)$$

in the limit of massless final-state leptons and $m_{Q_{i,j}}^2/M_{Q'}^2<<1$. Here, the approximate formula is obtained by expanding the cross section in powers of the relative velocity; $v_{\rm rel}$: $\sigma v_{\rm rel}\approx a_{\rm eff}+b_{\rm eff}v_{\rm rel}^2$, where $a_{\rm eff}=0$. The resulting relic density is found to be

$$\Omega h^2\approx\frac{1.07\times10^9x_f^2}{3\sqrt{g_*(x_f)}M_{\rm PL}b_{\rm eff}}, \quad (41)$$

where the present relic density is 0.1199 ± 0.0108 [19], $g_*(x_f\approx25)\approx100$ counts the degrees of freedom for relativistic particles, and $M_{\rm PL}\approx1.22\times10^{19}$ GeV is the Planck mass.

Numerical analysis:

We now perform a numerical analysis to satisfy the anomalies of the muon $g-2$, $B\to K^*\bar{\mu}\mu$, the constraints of the correct relic density, and the neutral meson mixing, as discussed above. We randomly select the input parameters as follows:

$$f_2=[-1,\sqrt{4\pi}],\quad g_{2,3}=\pm[0.01,0],$$
$$m_S=(10,1000)\ \text{TeV},\quad (M_{Q'},M_{L'})=(1.2m_s,5000)\ \text{GeV}, \quad (42)$$

where $1.2m_S$ is used to avoid the coannihilation processes among Q',L' and S, for simplicity. We show the allowed regions in Fig. 3, where the left(right)-hand figure represents the $f_2(m_S)--C_9$ plane, and the blue(red) points satisfy the muon $g-2$ in the range of $(26.1\pm8.0(16.0))\times10^{-10}$ in Eq. (35). The yellow(green) region denotes the experimentally allowed region [-1.22(-0.85),-0.18(-0.50)] at $1(2)\sigma$ in Eq. (38), where the black horizontal line inside the green region corresponds to the best fit value (BF). The left-hand plot suggests that f_2 is restricted to $[0.5,\sqrt{4\pi}]$ for both blue and red points. The right-hand plot implies that m_S is limited to [10,170(90)] GeV for red(blue) points.

5 Discussion and conclusions

We have proposed a new model with two flavor-dependent gauge symmetries: $U(1)_{B-L_1}$ and $U(1)_{B-L_2-L_3}$, in addition to the SM one, along with introducing three right-handed neutrinos to cancel gauge anomalies and several scalars to construct the measured fermion masses. We have examined the experimental bounds on the extra gauge bosons by considering the K and B meson mixings as well as the LEP and LHC experiments. The allowed parameter spaces for the masses and couplings of $Z'_{1,2}$ have been given. Even though all the regions are within the current exclusion bounds ($\sim$3 TeV) from the LHC [11], more stringent constraints or their discoveries will be found at ILC, with its sensitivity to the cut-off scale being around 50-100 TeV, which is stronger than the LEP constraints.

In addition, the possible effects on the flavor violating processes have been explored. Particularly, we have shown that the branching ratio of $\mu\to e\gamma$ for the case of $V_{\rm MNS}\approx U_{eL}$ can be large, which is testable by future experiments.

Finally, we have discussed the possibility of explaining the muon $g-2$, $B\to K^{(*)}\bar{\mu}\mu$, and dark matter candidate, by introducing vector-like fermions Q',L' and an inert complex boson S with appropriate charge assignments under $SU(3)_C\times SU(2)_L\times U(1)_Y\times U(1)_{B-L_1}\times U(1)_{B-L_2-L_3}$. We have also shown the allowed regions to satisfy all the anomalies and constraints, and

found $0.5 \lesssim f_2 \lesssim \sqrt{4\pi}$ for both blue and red points, and $10 \lesssim m_S \lesssim 170(90)$ GeV for red(blue) points. It is worth mentioning that the Z boson decay modes of $Z \to f_i \bar{f}_j$ at one-loop level could restrict our parameter space, where f_i represent all the SM fermions. It is expected that the sensitivities of these modes will further increase at future experiments, such as the CEPC [20], by several orders of magnitude.

This research was supported by the Ministry of Science, ICT and Future Planning, Gyeongsangbuk-do and Pohang City (H.O.).

References

1 H. Fritzsch and P. Minkowski, Annals Phys., **93**: 193 (1975), doi:10.1016/0003-4916(75)90211-0

2 P. Ko, T. Nomura, and H. Okada, Phys. Rev. D, **95**(11): 111701 (2017), doi:10.1103/PhysRevD.95.111701, arXiv:1702.02699 [hep-ph]; P. Ko, T. Nomura, and H. Okada, Phys. Lett. B, **772**: 547 (2017), doi:10.1016/j.physletb.2017.07.021, arXiv:1701.05788 [hep-ph]; Y. Tang and Y. L. Wu, Chin. Phys. C, **42**(3): 033104 (2018) doi:10.1088/1674-1137/42/3/033104, arXiv:1705.05643 [hep-ph]; C. W. Chiang, X. G. He, J. Tandean, and X. B. Yuan, Phys. Rev. D, **96**(11): 115022 (2017), doi:10.1103/ PhysRevD.96.115022, arXiv:1706.02696 [hep-ph]; C. H. Chen and T. Nomura, Phys. Lett. B, **777**: 420 (2018), doi: 10.1016/j.physletb.2017.12.062, arXiv:1707.03249 [hep-ph]; S. Baek, arXiv:1707.04573 [hep-ph]; L. Bian, S. M. Choi, Y. J. Kang, and H. M. Lee, Phys. Rev. D, **96**(7): 075038 (2017), doi:10.1103/PhysRevD.96.075038, arXiv:1707.04811 [hep-ph]; G. Faisel and J. Tandean, JHEP, **1802**: 074 (2018), doi:10.1007/JHEP02(2018)074, arXiv:1710.11102 [hep-ph]; K. Fuyuto, H. L. Li, and J. H. Yu, arXiv:1712.06736 [hep-ph]

3 S. Schael et al (ALEPH and DELPHI and L3 and OPAL and LEP Electroweak Collaborations), Phys. Rept., **532**: 119 (2013), doi:10.1016/j.physrep.2013.07.004, arXiv:1302.3415 [hep-ex]

4 M. Aaboud et al (ATLAS Collaboration), JHEP, **1710**: 182 (2017), doi:10.1007/JHEP10(2017)182, arXiv:1707.02424 [hep-ex]

5 L. Bian, H. M. Lee, and C. B. Park, arXiv:1711.08930 [hep-ph]

6 C. Patrignani et al (Particle Data Group), Chin. Phys. C, **40**(10): 100001 (2016)

7 F. Gabbiani, E. Gabrielli, A. Masiero, and L. Silvestrini, Nucl. Phys. B, **477**: 321 (1996), doi:10.1016/0550-3213(96)00390-2, [hep-ph/9604387]

8 H. Baer et al, arXiv:1306.6352 [hep-ph]

9 A. M. Baldini et al (MEG Collaboration), Eur. Phys. J. C, **76**(8): 434 (2016) arXiv:1605.05081 [hep-ex]

10 J. Adam et al (MEG Collaboration), Phys. Rev. Lett., **110**: 201801 (2013), arXiv:1303.0754 [hep-ex]

11 CMS Collaboration, Physics Analysis Summary CMS PAS EXO-12-061; G. Aad et al (ATLAS Collaboration), ATLAS-CONF-2013-017

12 W. Altmannshofer, S. Gori, M. Pospelov, and I. Yavin, Phys. Rev. Lett., **113**: 091801 (2014), doi:10.1103/ PhysRevLett.113.091801, arXiv:1406.2332 [hep-ph]

13 C. W. Chiang and H. Okada, arXiv:1711.07365 [hep-ph]

14 K. Hagiwara, R. Liao, A. D. Martin, D. Nomura, and T. Teubner, J. Phys. G, **38**: 085003 (2011), doi:10.1088/0954-3899/38/8/085003, arXiv:1105.3149 [hep-ph]

15 P. Arnan, L. Hofer, F. Mescia, and A. Crivellin, JHEP, **1704**: 043 (2017), doi:10.1007/JHEP04(2017)043, arXiv:1608.07832 [hep-ph]

16 S. Descotes-Genon, L. Hofer, J. Matias, and J. Virto, JHEP, **1606**: 092 (2016), doi:10.1007/JHEP06(2016)092, arXiv:1510.04239 [hep-ph]

17 D. S. Akerib et al (LUX Collaboration), Phys. Rev. Lett., **118**(2): 021303 (2017), doi:10.1103/PhysRevLett.118.021303, arXiv:1608.07648 [astro-ph.CO]

18 F. Giacchino, L. Lopez-Honorez, and M. H. G. Tytgat, JCAP, **1310**: 025 (2013), doi:10.1088/1475-7516/2013/10/025, arXiv:1307.6480 [hep-ph]

19 P. A. R. Ade et al (Planck Collaboration), Astron. Astrophys., **571**: A16 (2014), doi:10.1051/0004-6361/201321591, arXiv:1303.5076 [astro-ph.CO]

20 CEPC-SPPC Study Group, IHEP-CEPC-DR-2015-01, IHEP-TH-2015-01, IHEP-EP-2015-01